Airborne bacteria viability and air quality: a protocol to quantitatively investigate the possible correlation by an atmospheric simulation chamber

Virginia Vernocchi[1]*. Elena Abd El*[1,2]*, Marco Brunoldi*[1,2]*, Silvia Giulia Danelli*[1]*, Elena Gatta*[2]*, Tommaso Isolabella*[1,2]*, Federico Mazzei*[1,2*]*, Franco Parodi*[1]*, Paolo Prati*[1,2]*, Dario Massabò*[1,2]

[1] INFN, Sezione di Genova, via Dodecaneso 33, 16146 Genova, Italy

[2] Dipartimento di Fisica, Università di Genova, via Dodecaneso 33, 16146 Genova, Italy

Keywords: measure technique for bioaerosol, airborne bacteria, Atmospheric Simulation Chambers.

[*] *Corresponding author*: Federico Mazzei; federico.mazzei@ge.infn.it

Abstracts

Biological Particulate Matter or bioaerosol are a subset of atmospheric aerosol. They influence climate, air quality and health via several mechanisms which often are poorly understood. In particular, the quantitative study of possible relationship between bioaerosol viability and air quality or meteorological conditions is an open and relevant issue. The difficulty of retrieving such possible correlations by analyses of data collected during in-field campaigns, can benefit of targeted experiments conducted in well controlled conditions inside Atmospheric Simulation Chambers, ASCs. ChAMBRe (Chamber for Aerosol Modelling and Bio-aerosol Research) is an ASC in Genoa (Italy) designed and built to perform experimental research on bioaerosol. In this article we focus on bacteria viability. A multi-step protocol was developed and thoroughly tested: cultivation of a suitable bacteria population (*E. coli*), nebulization and injection in the chamber of viable cells, exposure and monitoring of the viability variation inside ChAMBRe, hold at selected conditions, and finally incubation and counting of the concentration of viable bacteria. The whole procedure showed an estimated lifetime of total (T) and viable (V) *E. coli* of about 153 and 32 minutes, respectively, and a V:T ratio lifetime of 40 ± 5 minutes when ChAMBRe is held in a reference "baseline" condition. The coefficient of variation of 13% shows how sensitive the protocol is also to changes in viability when the bacteria are exposed to other (e.g., polluted) conditions. First results showing a viability reduction observed exposing the *E. coli* strain to NO_X

concentrations and solar irradiation are presented and discussed. Present results pave the way to systematic studies aimed at the definition of dose-effect relationship for several bacteria strain at atmospheric pollutants.

1. Introduction

This article focusses on *bioaerosol,* the aerosol of biological origin. The major types of bioaerosols are primary and secondary biological aerosols and biogenic aerosols.

Primary biological aerosols (PBAs) refer to bioaerosols that are directly released into the atmosphere from biological sources, such as plants, animals, or microorganisms; these aerosols can be composed of various biological materials, including bacteria, viruses, fungi, pollen, spores, algae, or other organic particles (Ariya and Amyot, 2004; Fröhlich-Nowoisky et al., 2016).

Secondary biological aerosols (SBA) are the result of environmental processes or human activities that modify or transform primary biological aerosols. Unlike primary biological aerosols, SBA are not directly released from biological sources but are generated through secondary processes, like oxidation, condensation, etc., involving biological materials. SBA are fragments of larger biological particles, material released from cells (disruption, excretion…), nucleated biogenic gases, or cells "born" in the air from microbial multiplication (Morris et al., 2014, Ervens et Amato, 2020).

The PBAs vary in size depending on the specific biological material being aerosolized; they range from several nanometers (e.g., viruses, cell fragments) to a few hundred micrometers in aerodynamic diameter (e.g., pollen, plant debris) (Pöschl, 2005). Larger particles of biological material, such as large pollen grains or larger fragments of plants or insects, can be lifted into the air; however, due to their relatively high settling velocities, they tend to rapidly settle or deposit onto surfaces rather than remain suspended in the air for extended periods. As a result, these larger particles are typically not considered atmospheric aerosol particles (Després et al., 2012).

Among all the different bioaerosol microorganisms, bacteria are considered to play a significant role in the composition and dynamics of bioaerosols (Gong et al., 2020). They are ubiquitous in the atmosphere, and their presence and abundance can vary depending on factors such as location, season, and local environmental conditions: usually, over the land, the concentration in atmosphere is greater than 10^4 cells m^{-3} (Burrows et al., 2009) while our understanding of airborne microbes over oceans, is indeed limited compared to the knowledge we have about microbes in terrestrial

and aquatic environments. In a recent work (Mayol et al., 2014), the airborne prokaryotic abundance over the North Atlantic ocean ranged from about 3000 to 20000 prokaryotes m^{-3} (average about 8000 cells m^{-3}).

Bacteria, as small airborne particles or aerosols, can have relatively long atmospheric residence times compared to larger particles. This is due to their small size and low settling velocity, which allows them to remain suspended in the air for prolonged periods. (Després et al., 2012). Airborne bacteria may be suspended as individual cells or attached to other particles, such as soil or leaf fragments, or found as agglomerates of many bacterial cells (Lighthart, 1993). For this reason, whereas individual bacteria are typically on the order of ~1 μm or less in size, the median aerodynamic diameter of particles containing culturable bacteria at several continental sites has been reported to be ~ 2 - 4 μm (Shaffer and Lighthart, 1997; Wang et al., 2007). Even if up to now several works have contributed to the identification of bacterial diversity in the atmosphere (Amato et al., 2007; Burrows et al., 2009; Després et al., 2012, Romano et al., 2019), it remains difficult to establish a clear picture of the actual abundance and composition of bacteria in the air. Numerous studies have suggested that the presence of bacteria in the atmosphere can have significant implications for cloud formation, atmospheric chemistry, microbial biogeography, and climate. As a matter of fact, bacteria can serve as ice nucleating particles and cloud condensation nuclei, influencing the precipitation processes, affecting cloud lifetime, optical properties, and climate patterns (Bauer et al., 2003; Morris et al., 2004; Sun and Ariya, 2006; Möhler et al., 2007). In particular, bacterial viability, the proportion of viable to total bacteria concentration, can act as Cloud Condensation Nuclei (CCN) thanks to the hygroscopic properties of their surfaces (Delort et al., 2010). Additionally, the near-surface atmosphere's viable bacteria can have a significant impact on human health, including allergies, acute toxic effects, and infections (Bolashikov and Melikov 2009).

Since bacteria have also been shown to metabolize within cloud droplets, some authors have proposed an impact on the chemistry of cloud droplets and air (Fankhauser et al., 2019; Jaber et al., 2021, 2020; Khaled et al., 2021). Finally, the presence of bacteria in the atmosphere can influence microbial biogeography (Martiny et al., 2006) by facilitating long-distance dispersal and the establishment of microbial populations in new environments.

Bacteria can enter the atmosphere as aerosol particles from various surfaces, including soil, water, and plant surfaces (Burrows et al., 2009). Once in the air, they are carried upwards by air currents

and may remain in the atmosphere for many days before being removed by wet or dry deposition onto surfaces. Indeed, the mechanisms that govern the transport, survival, and activity of bacteria in the atmosphere are complex and multifaceted. Understanding these mechanisms is crucial for various scientific disciplines, including microbiology, atmospheric science, and public health. This complexity is related to some key factors such as aerosolization, transport and dispersion, survival, hygroscopicity, interactions with other particles, droplet nucleation, deposition, activation of ice nucleation, impacts on cloud formation and chemistry and all these processes are indeed intertwined (Amato et al., 2023).The interactions between bacteria and their living environment, as well as the atmospheric conditions, play crucial roles in determining their behavior and impacts on climate (Deguillaume et al., 2008) and, consequently, on health.

Atmospheric Simulation Chambers (ASCs) have been widely used to study chemical and photochemical atmospheric processes, but the high versatility of these facilities allows for a wider application covering all fields of atmospheric aerosol science. For example, a consistent improvement in characterizing bioaerosols, in understanding the mechanisms affecting their behavior in the atmosphere and finally in elucidating their impacts, can be obtained using atmospheric chamber facilities, where transdisciplinary studies addressing atmospheric physics, chemistry, and biology issues are possible.

In the last decades, the use of atmospheric simulation chambers has been much more focused on the potential interest of bioaerosol as ice nuclei and cloud condensation activity (Möhler et al., 2008b; Bundke et al., 2010; Chou, 2011). Few studies have investigated bacterial survival and activity using simulation chambers, and some of them are old (Wright et al., 1969 Ehrlich et al., 1970; Krumins et al., 2014). Recently, addressing the public health concerns related to bioaerosol contamination has led to increased research efforts focusing on the survival and transformation of bioaerosols in the atmospheric environment. Innovative chamber studies have been initiated to investigate these questions and gain insights into the behavior of bioaerosols (Amato et al, 2015; Brotto et al, 2015). These works have led to the development of a new dedicated simulation chamber, ChAMBRe (Massabò et al., 2018). The chamber has been installed at the National Institute of Nuclear Physics in Genoa (IT) in collaboration with the Environmental Physics Laboratory at the Physics Department of the University of Genoa. ChAMBRe is also a National Facility of the constituting ERIC-ACTRIS, the worldwide largest research infrastructure to study atmospheric phenomena, set up by the European Union on April 25th 2023 (CID, 2023). The main

scientific target at ChAMBRe, is the description of biological micro-organisms behavior in the atmosphere, aiming to a deeper understanding of the still unclear mechanisms that control the evolution of bioaerosols in atmosphere, in particular their bacterial components. The long-term goal is the parameterization of survival and activity of bioaerosols to develop specific tools to be implemented in chemical transport models (e.g., CAMx, Wagstrom et al., 2008) presently limited to treat transport and chemistry of gaseous and not-biological aerosol species.

This article gives all the details of the present status and capability of the ChAMBRe facility and introduces a multi-step, interdisciplinary procedure assessed to perform quantitative studies on the impact of different pollutants on bacteria viability. Preliminary results are also shown to illustrate the sensitivity of the experimental procedures developed at ChAMBRe that pave the road to systematic investigations on different strains and air quality conditions.

2. Material and Methods

Since the beginning of 2017, ChAMBRe has been one of the nodes of the EUROCHAMP-2020 network with specific tasks on bio-aerosol studies. From the date of installation, on ChAMBRe control and acquisition system has been enriched with a wide range of equipment aimed at monitoring and controlling the processes occurring inside the chamber. In addition, most efforts have been devoted to developing protocols to produce, inject, expose and collect bio-aerosols, to maximize the experiments reproducibility.

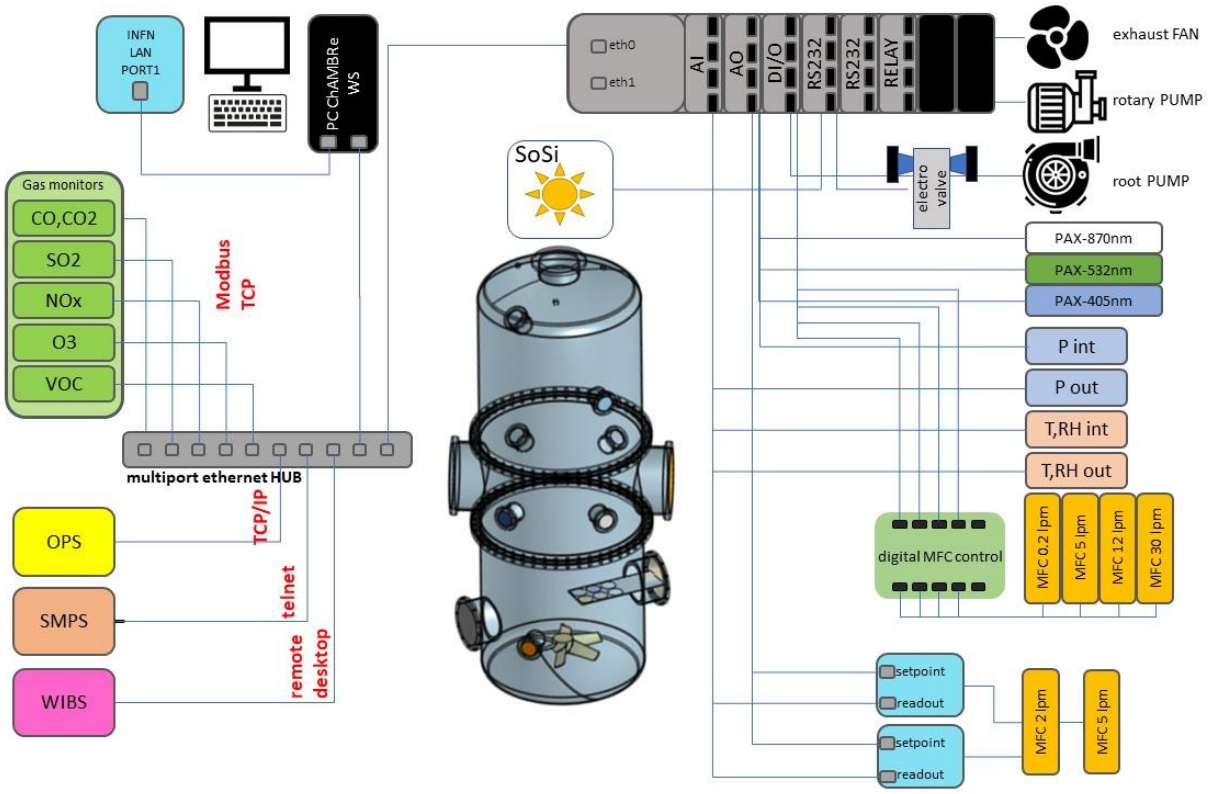

Figure 1: ChAMBRe layout

Briefly, ChAMBRe (Massabò et al., 2018) has a cylindrical shape with domed bases. It has a maximum height and diameter of 2.9 and 1 m, respectively, and a total volume of about 2.2 m^3. The main body is divided into three parts (two domed cylinders connected by a central ring) equipped with several flanged apertures of different diameters matching the different types of fitting for instrument interfacing.

To favor the mixing of the gas and aerosol species, a fan is installed at the bottom of the chamber. It is a standard venting system with a particular pass-through designed and built at INFN-Genoa to ensure the vacuum seal. The fan speed can be regulated by an external controller and set up to 50 Hz in steps of 0.1 Hz.

One of the two flanges in the bottom part is connected through a pneumatic valve to a smaller horizontal cylinder (length about 1 m), which hosts a movable tray designed to move specific samples inside the chamber. The samples are typically Petri-dishes for bacteria collection inside the chamber during the experiments: they can remain exposed for the whole experiment or for a selected time interval controlled by the user. A custom-made side flange has been worked in the central ring of the main body of the chamber. The large tipper tailgate allows the introduction and

positioning of bulky sensor devices for testing and calibration purposes. The flange features a small window for visual inspection and four vacuum feedthrough connectors to power and communicate with devices inserted in the chamber.

ChAMBRe is equipped with a composite pumping system (rotary, root and turbo pump) which can evacuate the internal volume to a level of about 5×10^{-4} mbar. The return to atmospheric pressure can proceed by flowing ambient air inside the chamber through a five-stage filtering/purifying/drying inlet system including an absolute HEPA filter and a zeolite trap or using synthetic air from a cylinder (reducing the relative humidity close to zero).

Two types of UV lamps are permanently installed inside the chamber. A 58 cm long lamp (W = 60 W, λ = 253.7 nm; UV-STYLO-F-60H, Light Progress Srl) is inserted through a custom side flange to sterilize the chamber volume without producing ozone after any experiment involving bioaerosol. A second type of lamp, producing UV radiation at $\lambda < 240$ nm, can be inserted through one of the ISOK100 flanges of the central ring to generate ozone.

A set of two pressure gauges is used to measure the atmospheric pressure inside (range 5×10^{-4} - 10^{3} mbar) and outside (range of 5×10^{-2} - 10^{3} mbar). ChAMBRe internal temperature and relative humidity are continuously measured by a sensor located in the upper ISO-K100 flange on the top dome.

Supervised injection of known volumes of different gas species inside the chamber is made by a set of software-controlled digital mass flow controllers (MFC) ranging from 5 to 30 lpm full-scale manufactured by Bronkhorst®. Two 5-lpm MFCs are designed for injection of CO_2 and other gases (i.e. SO_2, CO, NO and NO_2), respectively, whose concentration in the chamber can be selected by the operator (ppm or ppb units); a PID (Proportional–Integral-Derivative) controller, using the gas concentration values read from the corresponding gas analyzer, keeps the gas concentration in ChAMBRe constant during the experiment.

A 30-lpm MFC regulates the injection of dry air inside the chamber. In this case, the PID controller (using the ChAMBRe pressure values measured by pressure sensor mentioned above) allows to maintain a pre-defined pressure gap between inside and outside the chamber. A 12-lpm and a 0.2-lpm MFCs are dedicated to the injection of known volumes of air and fuel, respectively, inside the burning chamber of a Mini Inverted Soot Generator (Argonaut Scientific Corp., Edmonton, 49 AB, Canada, Model MISG–2). The MISG can be connected to an inlet flange of ChAMBRe for the study of the properties of soot particles exposed and maintained in different conditions or to

study the effects of soot particles. The input air flow of the nebulizers (see Par. 2.2), responsible for the crucial process of bacteria injection inside the chamber, is regulated by an analog 5-lpm full-scale MFC (EL-Flow®).

2.1 Instruments permanently connected to the chamber.

The concentration of several gaseous pollutants potentially present inside the chamber can be monitored by a set of calibrated gas detectors manufactured by ENVEA®: non-dispersive Carbon monoxide and dioxide analyzer (CO12e), Ozone analyzer (O342e), Sulfur dioxide analyzer (AF22e), chemiluminescent Nitrogen Oxides analyzer (AC32e) and Gas chromatography VOC analyzer (VOC72M). Details on the quoted monitors are provided in Supplement S1.

A custom solar simulator manufactured by Sciencetech™ has been installed on the top of the upper dome of the chamber. The top ISO-K250 flanged aperture has been appropriately modified by inserting a dedicated quartz window (diameter = 25 cm) with a high degree of transmittance (> 95 %, with $300 < \lambda < 900$ nm) and reflectance (< 1.5% with $300 < \lambda < 900$ nm) to the solar spectrum radiation. The system consists of two main sections: the light source and the power supply. The light source, a 1600 W Xenon Shor Arc lamp (Sciencetech™ - XE1600), is mounted inside a dedicated housing where a set of optical lenses and mirrors deflects the light beam perpendicularly to fit the quartz window aperture. A set of filters are available to intercept the light beam and cut-off selectable portions of the spectrum before entering the chamber. In particular, the simulator can be fitted with a low-pass optical filter, designed to cut off a portion of the spectrum in the infrared (IR) region. Alternatively, the optical absorption of the atmosphere can be simulated by using a dedicated filter (AM1.5G 3 × 3" air mass filter, Sciencetech™), which cuts off selected bands to mimic the light interaction of an air mass coefficient of 1.5 (i.e., an optical path length that is 1.5 times that of light traversing the atmosphere at the zenith). Figure 1 shows the impact of the available filters on the light spectrum sent to the chamber. The nominal maximum irradiance provided by the Solar Simulator without any filter is about 2.4 SUN, actually 2,424 W m^{-2}, corresponding to about 119 W passing through the quartz window on the ChAMBRe top dome with the AM1.5 filter mounted inside the solar simulator.

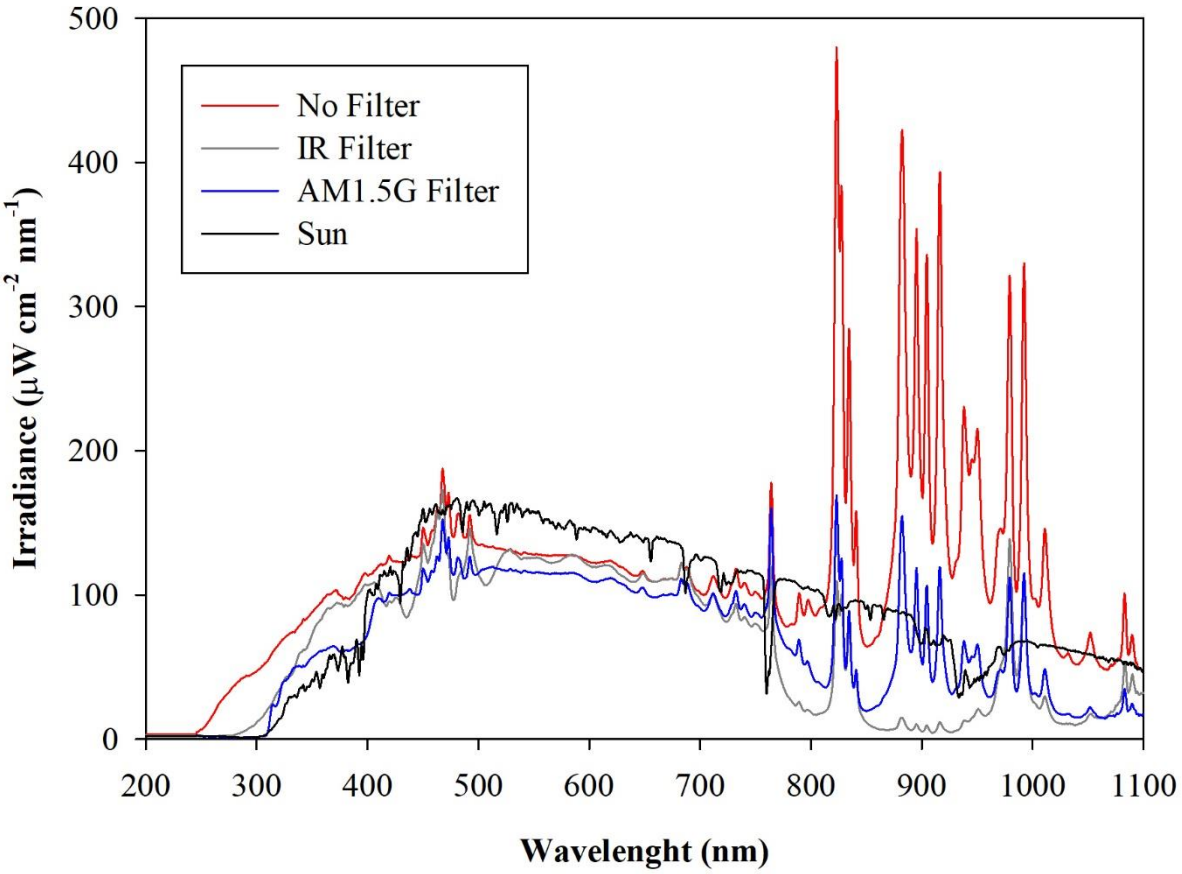

Figure 2: Irradiance vs wavelength measured with a calibrated Avantes ULS2048CL-EVO spectrometer directly at the exit of the Solar Simulator with and without the available filters. The spectrum labelled "Sun" has been measured on a springtime sunny day in the terrace of the Physics Department in Genoa, Italy. The uncertainties of irradiance (not reported in the graph) are ± 10% from 200 to 350 nm and 5% from 350 to 1100 nm.

The solar simulator is also equipped with a set of four neutral density optical filters, to reduce the light intensity entering the chamber. These filters provide an attenuation of 19%, 34%, 50% and 71% of the lamp power, respectively, and can be fitted two at a time on the device, offering a minimum transmittance of 7%. The neutral density filters do not significantly alter the shape of spectrum of the transmitted light, attenuating the optical power uniformly (see Supplement S2, Figure S2).

The radial distribution of the optical power measured inside the chamber volume is shown in Figure 3, as a function of the distance along a cross-sectional diameter in the center of ChAMBRe. The light intensity has a strong peak at the center of the diameter, where the optical power is more

than six times that close to the walls. To obtain the total light intensity irradiated by the lamp in the chamber volume, the measured data points were fitted with a double gaussian function, which was then integrated in cylindrical coordinates, exploiting the symmetry of the light beam. The resulting intensity is 160 ± 6 W with the lamp set at full power (power supply set at 105% of the nominal value) and no optical filter. The total intensity with the AM1.5 filter is 94 ± 4 W, while with the IR filter the total integrated intensity is 81 ± 4 W. With respect to the irradiance measured directly at the Solar Simulator output, the value inside the chamber shows just a loss of about 20% (likely due focusing/collimation). It must be noted that, at the maximum power and no-filter, the irradiance measured on the middle plane of ChAMBRe is about 0.2 SUN, this almost corresponding to the dilution given by the ratio of the surfaces of the top quartz window (diameter of 25 cm) and of the chamber (diameter of 100 cm).

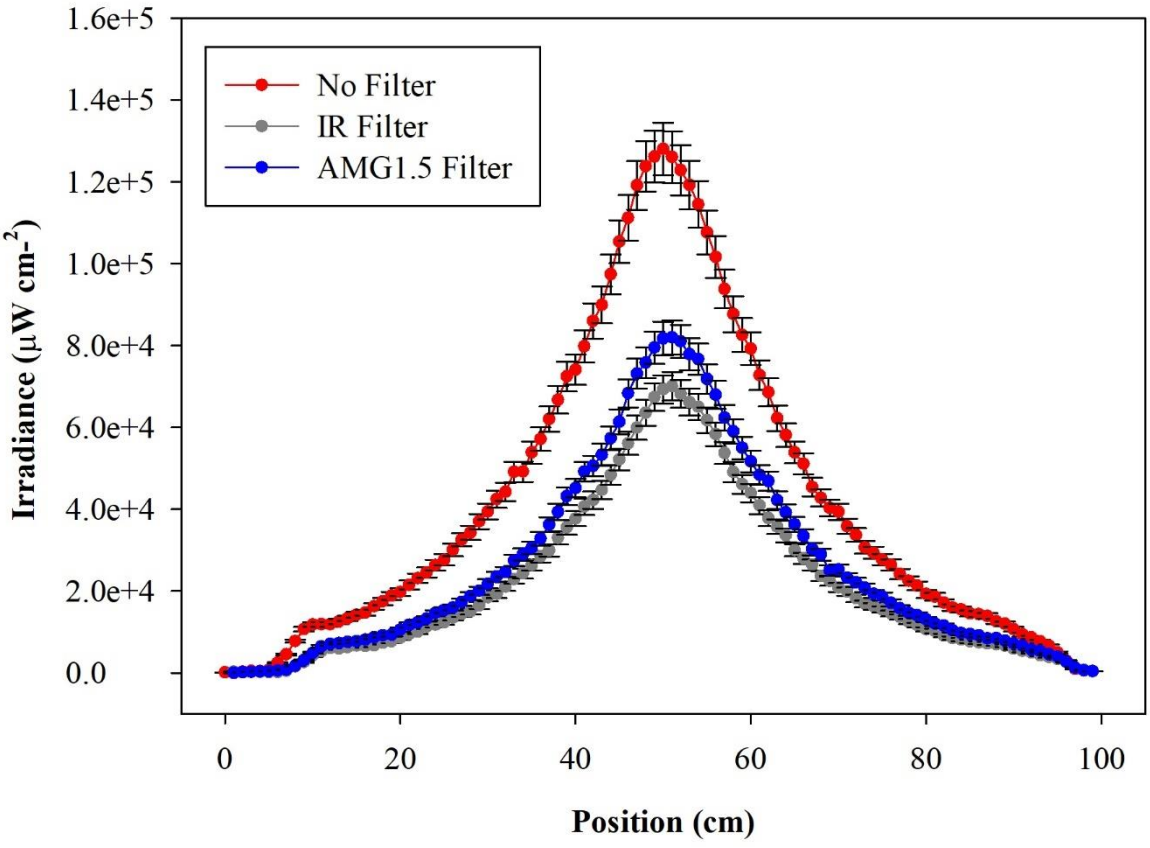

Figure 3: Irradiance vs wavelength measured with a calibrated Avantes ULS2048CL-EVO spectrometer along a diameter at the center of the ChAMBRe volume, with and without the available optical filters. The center of the chamber is at position=50 cm.

Particle concentration and size distribution inside ChAMBRe are real-time monitored by a Scanning Mobility Particle Sizer (SMPS; TSI Inc., model 3938), in the range of 10 – 1000 nm, and an Optical Particle Sizer (OPS; TSI Inc.; model 3330) in the range 0.3 - 10 μm. The SMPS is formed by three components: a neutralizer (i.e., a bipolar diffusion charger), a differential mobility analyzer (DMA, series 3080) and a condensation particle counter (W-CPC, model 3789), from TSI Inc. The model 3088 Neutralizer uses a low-energy (< 9.5keV) soft X-ray source to generate high concentrations of both positive and negative ions to bring the aerosol to a defined, steady-state charge distribution. The DMA is available with two different columns: model 3081 Long DMA, which provides the widest size range of 10-1000 nm, and the model 3085 Nano DMA, which covers the range of particle diameter from 2 and 150 nm. In a DMA, an electric field is created and the airborne particles drift in the DMA according to their electrical mobility. Particle size is then calculated from the mobility distribution. In the CPC, downstream of the DMA, the particle size is increased by water condensation on their surface and then the particles are optically counted. The maximum measurable concentration can reach 2×10^5 particles cm^{-3}. The SMPS working airflow ranges between 0.2 and 1.5 lpm.

The Model 3330 OPS is an optical particle sizer spectrometer that provides measurement of particle number concentration and particle size distribution based on single particle counting technology. The OPS has an inlet flow rate of 1.0 lpm ± 5% and measures particles from 0.3 μm to 10 μm in 16 user-adjustable size channels (particles above 10 μm are counted but not sized). The OPS 3330 works on the principle of optical scattering from single particles. The OPS uses a laser beam (λ = 660 nm) and a detector to detect particles passing through a sensing volume illuminated by the laser. Particle pulses are counted individually and binned into 16 channels up to their pulse heights. The OPS is factory calibrated using different monodispersed Polystyrene Latex particles (PSL) for size classification; size resolution is 5% at 0.5 μm following the procedure described in the ISO 21501-1 normative. Particles exiting the chamber are trapped by a gravimetric filter for possible after sampling chemical analysis.

A Waveband Integrated Bioaerosol Sensor (WIBS-NEO, Droplet Measurement Technologies®) has been integrated in the ChAMBRe particle monitoring system to measure bio-aerosols concentration. The instrument uses two UV filtered flashlamp sources (λ = 280 nm and λ = 370 nm) to excite fluorescence in individual particles (Lieberherr et al., 2019). Detection wavebands

have been selected to optimize detection of common bioaerosol components and let the user discriminate between different types of biological micro-organisms (bacteria, fungi, pollen, etc.). The massive amount of data generated by the WIBS during the experiments at ChAMBre through a list-mode off-line analysis, has made necessary to develop a dedicated software tool, written in Igor 8.0 (Wavemetrics, Inc.) language, aimed at implementing a multi-parametric data reduction and to retrieve the airborne bacteria/bioaerosol concentration inside the chamber as a function of time. Starting from the raw data, the Igor procedure first sets a background threshold for the particle fluorescence intensity and groups the particles into three channels (A, B, C) and their relative intersections (AB, AC, BC, ABC) according to their presence within the three fluorescence detection waveband groups (FL1, FL2, FL3), following the terminology adopted in the WIBS (Lieberherr et al., 2019). Then, for signal-background separation purpose, fiducial cuts are applied on scatter plots (Fluorescence Intensity vs Particle Size) relative to particles belonging to channel A, which is known to be mainly populated by particles showing a bacteria-like fluorescence emission. Examples of the scatter plots are reported in Figure 4 where the region of interest of the signal (*E. coli* bacteria) is well separated from the background region.

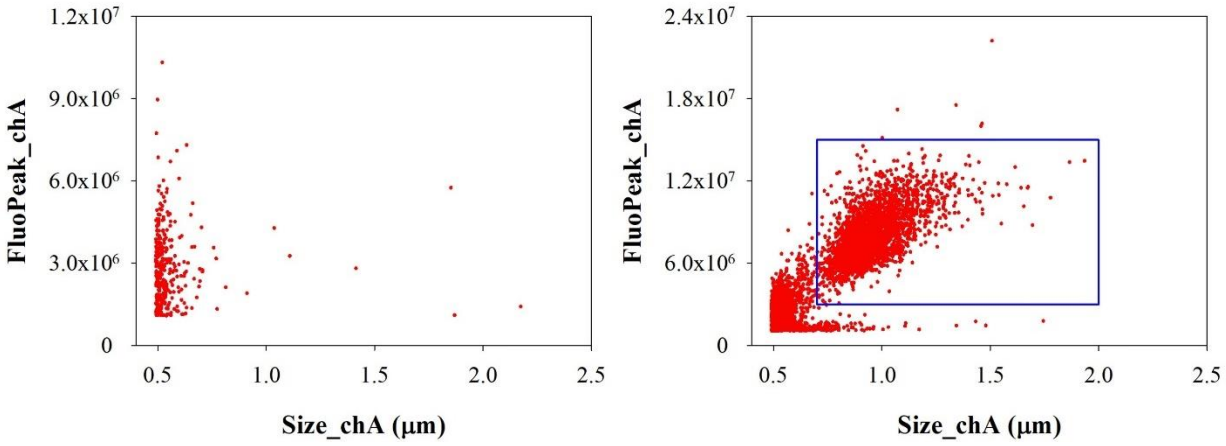

Fig 4: Size distribution of particles in channel A. Left: background measured without any bacteria injected in ChAMBRe. Right: particles population after *E. coli* injection. The particles inside the blue rectangular region of interest are identified as *E. coli*.

Finally, the whole analysis is cycled over user-selectable time intervals to retrieve the time-resolved particle concentration during the whole experiment. Figure 5 shows the time series of *E. coli* concentration inside the chamber during a typical experiment.

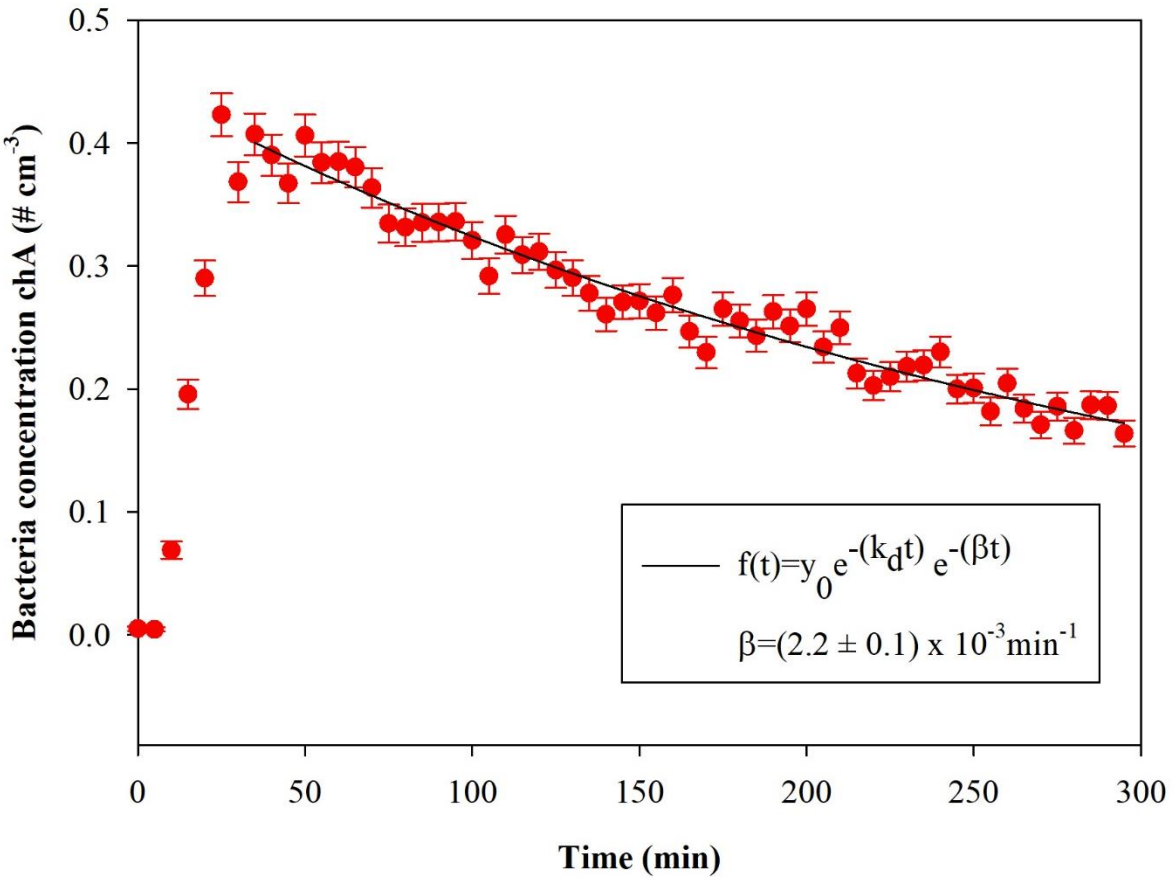

Figure 5: Temporal trend of *E. coli* particles inside the chamber; t = 0 is the injection start. The curve fit is also shown, where β is the particle loss rate coefficient and k_d is the dilution factor (here $k_d = 1.02 \times 10^{-3}$ min^{-1}). The error bars are the standard deviations calculated following the Poisson statistics.

Optical properties (i.e., absorption, extinction and scattering coefficients) of particles suspended inside the chamber can be measured online by photoacoustic extinction meters (PAXs; Droplet Measurement Technologies) at three wavelengths: λ = 870, 532 and 405 nm. The PAX directly measures in-situ light absorption and scattering of aerosol particles, from which it derives extinction, single scattering albedo and black carbon mass concentration (Vernocchi et al., 2022). PAX uses a modulated diode laser to simultaneously measure light scattering and absorption. The standard infrared, 870 nm wavelength option, is highly specific to black carbon particles, since there is relatively little absorption from gases and non-BC aerosol species at this wavelength. A nominal 1 lpm aerosol sample flow is drawn into the PAX using an internal vacuum pump controlled by two critical orifices. The flow is split between the two distinct measurement regions: a nephelometer, for the light scattering measurement and a photoacoustic resonator for

the absorption measurement. Absorbing particles heat up and quickly transfer heat to the surrounding air. A sensitive microphone detects the pressure waves produced by the heating, whose intensities are interpreted to infer the particle absorption coefficient (Moosmüller et al., 2009). In the nephelometer, a photodiode set at 90° with respect to the beam detects the radiation reflected by the sampled particles. The scattering measurement responds to all particle types regardless of chemical makeup, mixing state, or morphology.

Acquisition and control of the instruments connected to ChAMBRe is handled by a National Instruments™ based system made up of a main controller (NI9057 cRIO) and several modules (C Series modules), which allow communication with the peripheral devices via analog, serial, and ethernet data transfer protocols. The operator interaction with the sensor network is demanded to a single NI-LabVIEW™ SCADA (Supervisory Control And Data Acquisition) custom application which provides the user with a global data overview and a full real-time control above all the instruments parameters via a user-friendly human-machine interface (HMI). In Supplement S1 (Figure S1), a screenshot of the main panel of the SCADA application is shown.

2.2 Other equipment for specific applications/experiments

Aerosols to be used in ChAMBRe experiments can be generated in different ways, depending on the specific application. The Flow-Focusing Monodisperse Aerosol Generator (FMAG, TSI Inc. model 1520) can be used to produce monodisperse particles in the diameter range 0.8 - 12 μm, starting from both liquid and solid materials. The MISG is used to produce soot particles from the controlled combustion of different gaseous fuels (Vernocchi et. al 2022).

Three nebulizers, designed for bioaerosol applications, are also available: the Collison nebulizer, the Blaustein Atomizing Modules (BLAM), and the Sparging Liquid Aerosol Generator (SLAG), all manufactured and distributed by CH TECHNOLOGIES Inc. The performances of the three nebulizers in connection to the injection of viable bacteria in the chamber have been previously investigated and described in (Danelli et al., 2021).

Bacteria injected inside ChAMBRe can be collected by different methods. All the methods described below allow to perform offline analyses. A cylindrical horizontal volume is connected to the chamber by an ISO-KF250 pneumatic valve; this volume can be alternatively opened or closed without perturbing the inner atmosphere thanks to another ISO-KF250 pneumatic valve. Inside the cylinder, there is a sliding tray that can be inserted in ChAMBRe by an external manual

control, to minimize the risk of contamination. The tray can host up to six Petri dishes (diameter 10 cm, each) to collect bacteria (or in general BPA) directly by gravitational settling. In addition, bacteria can be collected on solid medium (i.e., Petri dishes filled with culture medium) by the active sampling by an Andersen impactor (Single Stage Andersen Cascade Impactor, TISCH Environmental) working at a fixed air flow of 28.3 lpm, supplied by a dedicated pump. The impactor is connected to the chamber by ISO-K flanges. Moreover, bioaerosol can be collected through liquid impinger, (Flow Impinger, Aquaria srl), filled with 20 ml of sterile liquid solution, . Such a device can be easily connected to the chamber volume through the ISO-K flanges. Impinger operates at a constant airflow of 12.5 lpm (e.g., by a low-capacity pump: Model LCP5, Copley Scientific). Finally, aerosol suspended in the chamber can be also collected on filters (i.e., quartz fibre, PTFE, cellulose). Sampling is managed by a low-volume particulate matter sampler, setting the air flow in the range 10 – 50 lpm.

2.3. Equipment to manipulate bioaerosol

A biological laboratory with specific instrumentation for isolating and maintaining bacterial cells culture is part of the ChAMBRe facility:

- Biosafety cabinet, and laminar flow hood, Miniflow Linear blue air Aquaria, (Milano, Italy). It is used to provide a contamination-free working environment for the workers. A laminar flow filters the air and traps dust particles and microbes for providing a sterile working environment in the stainless-steel cabinet. The hood is equipped with HEPA filter and an UV-light lamp allows the sterilization of the illuminated surfaces inside the hood.
- Centrifuge MPW-352 MPW MED Instruments (Warsaw, Poland) used to separate particles from a homogeneous solution through rotational movement and centrifugal acceleration, causing sedimentation of its components. The MPW-352 has a swinging-bucket rotor that swings out when centripetal force is applied and holds the pellet at an approximate 90° angle relative to the angle of rotation.
- Spectrophotometer Shimadzu 1900, designed for liquid samples, is a double-beam UV-Vis Shimadzu Corporation, Japan. This instrument measures intensity as a function of light source wavelength. For each wavelength of light passing through the spectrometer, the intensity of the light passing through the sample cell is measured. The biological

applications include measurement of substance concentration such as protein, DNA or RNA, growth of bacterial cells, and enzymatic reactions.

- Shaker incubator, designed for liquid samples, with orbital rotation movement SKI 4 ARGOLAB, Carpi MO – Italy. It provides a controlled environment for samples to grow and develop while also providing mechanical agitation to mimic the natural movement of cells in their environment. Shaking can be used to promote the growth and development of cells and microorganisms to increase the oxygen supply to the cells. The oxygen is an important factor that can affect the growth and metabolism of cells. By shaking the culture, it is possible to increase the oxygen supply to the cells by increasing the diffusion of oxygen into the media.

Quantom Tx microbial cell counter Logos Biosystems, South Korea. This automated cell counter can detect individual bacterial cells in a liquid sample. The instrument provides counting of the total number of cells in the suspension using fluorescent probe. It captures images of (10-fields) fluorescence-stained cells. The optimal concentration range of count is $5 \times 10^5 – 5 \times 10^8$ cells ml^{-1} and the size range of the count cells is between 0.3 and 50 μm. To evaluate the uncertainty on the bacteria count (QT x TOT), we repeated the measurement on the same sample 10 times, and we found a results repeatability of 5%. This uncertainty is much higher than the statistical error of total counting (assuming the Poisson statistic), and, for this reason, we adopted a 5% uncertainty to all Quantom Tx counts. The sample is prepared from the bacterial suspension in physiological solution immediately before injection; for counting the total number of cells, three different solutions to 10 μl of the initial suspension are added: *Total Cell Staining Dye*, *Total Cell Staining Enhancer* and *Loading Buffer I.* The first added is the *Total Cell Staining Dye,* a membrane-permeable fluorescent dye, which is capable of binding to nucleic acids in viable and non-viable cells and allows the detection of Gram-positive and Gram-negative bacteria. This probe has an excitation wavelength of $\lambda = 484$ nm, and it emits $\lambda = 504$ nm. The second solution used is the *Total Cell Staining Enhancer* to guarantee a better cells penetration by the probe and to obtain a uniform background during the images acquisition by Quantom Tx. The sample must be incubated in the dark at 37°C for about 30 minutes to favor the penetration of the fluorescent dye into the cells. Finally, the *Loading Buffer I* is added and used to uniform the distribution and the sedimentation of bacterial cells in the counting stands. The slide, after being centrifuged at 300 RCF for 10 minutes, is inserted in the specific support in the counter and then illuminated with a

lamp at $\lambda = 470$ nm with a bandpass of 30 nm. The light power can be set to nine levels of intensity (labelled from 1 to 9): in our experiments, the best results are obtained selecting the intensity of 5 for counting total cells.

2.3.1 Bacteria cultivation, injection and monitoring

The bacteria strain so far used to perform experiments at ChAMBRe is *Escherichia coli* (ATCC® 25922™), Gram-negative, purchased by Thermo Scientific™ Culti-Loops™. *E. coli* is rod-shaped, about 1–2 μm long and about 0.25 μm in diameter (Jang et al., 2017). It is a common inhabitant of the gastrointestinal apparatus of warm-blooded animals, including humans. This strain is a non-pathogen proxies of typical atmospheric bacteria, extensively used as model organisms in microbiology and molecular biology fundamental and applied studies (Lee et al., 2002; Lee and Kim, 2003).

Bacterial growth is a complex process that involves several distinct phases. The increase in numbers or bacterial mass can be measured as a function of time under culture conditions where the nutrients and environmental conditions are controlled. Several distinct growth phases can be observed within a growth curve such as the lag phase, the exponential or log phase, the stationary phase, and the death phase. The first stage, the lag phase, occurs when bacteria are not dividing but are metabolically active. During the lag phase of the bacterial growth cycle, the synthesis of RNA, enzymes, and other molecules occurs. The length of this phase depends on the type of bacterial species, culture medium, and environmental factors. The log phase is an exponential phase characterized by rapid growth, with binary fission. The number of new bacteria appearing per unit time is proportional to the present population. If growth is not limited, doubling will continue at a constant rate, so both the number of cells and the rate of population increase doubles with each consecutive period. Exponential growth cannot continue indefinitely, however, because the medium is soon depleted of nutrients and enriched with catabolites. (Maier R. et al., 2008). The stationary phase is due to a growth-limiting factor; this is mostly depletion of a nutrient, and/or the formation of inhibitory products such as organic acids. Instead during the death phase, the number of living cells decreases exponentially. Bacteria run out of nutrients and die although the number of cells stays constant. The decline phase is brought by exhaustion of nutrients, accumulation of toxic products, and autolytic enzymes. The microbial growth curve is a record of the countable cells determined at certain time intervals during the population's evolution. In our

work, the calibration curve was figured out converting the rate growth from optical density (OD) values to CFU (Colony Forming Unit) ml^{-1}, as explained in detail below.

The day before the experiment, bacteria cells are scraped off agar medium, where they are cultivated, using sterile plastic loops and suspended in a sterile, non-selective culture broth medium Tryptic Soy Broth (TSB) and incubated overnight at 37 °C. The day after, 3 ml of the bacteria culture is diluted in 30 ml of new broth medium, and the suspension is incubated again at 37 °C. At intervals of about thirty minutes, the OD of the bacterial solution is measured by the spectrophotometer at $\lambda = 600$ nm; OD_{600nm} allows to estimate the concentration of bacterial cells in the liquid and tracking the growth. The mid-exponential phase is typically reached when OD_{600nm} is about 0.5 (Mytilinaios et al., 2012; Hall et al., 2014). For selected OD values, the bacterial concentration was also measured/referred as Colony Forming Units (CFU). The bacteria solution must be diluted several times to obtain not overlapping colonies on Petri Dishes: 100 µl of bacterial solution is added in 900 µl of sterile saline solution (NaCl 0.9 %), then diluted again as many times as the theoretical concentration (calculated using the OD value) required; 100 µl of the last dilution is spread in duplicate on an TSB agar and incubated overnight at 37 °C. The next day the concentration of culturable cells is measured by counting the colonies formed and multiplying by the proper dilution factor to retrieve CFU concentration in the original solution. Data, obtained by CFU counting on agar plates, are weighted averaged and used to figure out the uncertainty (standard error of weighted mean) of the bacterial concentration in the solution. The weights are the relative uncertainties of CFU number on agar plates following the Poisson statistics.

Several sigmoidal functions have so far been adopted to describe a bacterial growth curve. The literature on these models is well known and is used in various contests: plants, bird growth, fish and other animals, cancers and bacterial growth (Kathleen M. et al., 2017). We tested the fits to our *E. coli* growth curves by Logistic, Gompertz, and Richards models. (Birch C.P. 1999; Baty F. and Delignette-Muller M.L. 2004). The logistic function model is used specifically to describe growth of microorganisms, as a function of nutrient depletion (Daniel E. W. et al 2003) and it was demonstrated to be the best fit for modeling bacteria (Akin et al 2020; Annadurai G. et al. 2000). Here, the results of the logistic fit only are shown. The logistic equation was written as:

$$y(t) = \frac{y_0}{1 + e^{-b(t-t_0)}} \quad (1)$$

where y indicates the bacteria concentration in the solution, y_0 is the saturation value, b is the maximum specific growth rate and t_0 is the time at the inflection point.

We followed the growth of *E. coli* in suspension culture for about 8 hours from lag phase to horizontal asymptote and the OD_{600nm}, the total number of *E. coli* (QTx TOT), measured with Quantom TX and the CFU ml^{-1} values are reported in Figure 6. The values of reduced chi-squared, (χ^2), y_0, b and t_0 of the logistic fit for OD_{600nm}, QTx TOT and CFU ml^{-1} are reported in Table 1.

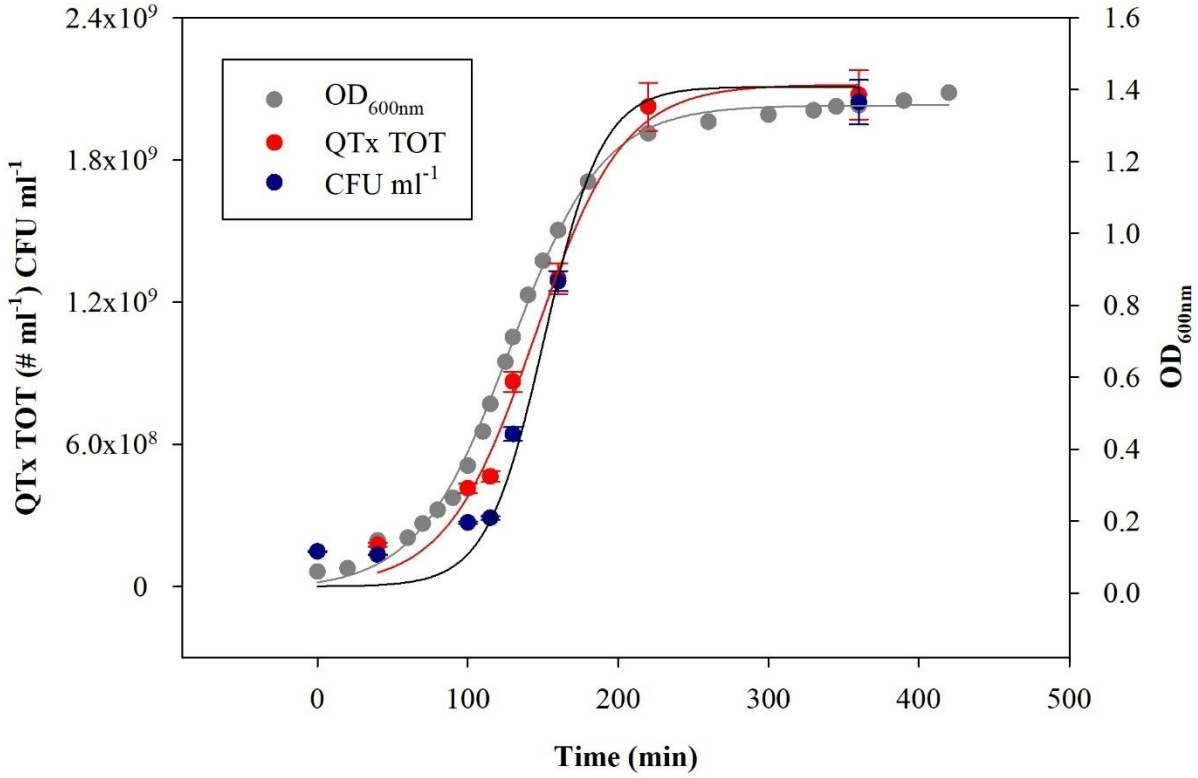

Figure 6: Grow curve for *E. coli*: optical density (OD_{600nm}), total number of *E. coli* measured by QUANTOM-TX (# ml^{-1}) and the corresponding bacteria concentration (CFU ml^{-1}) vs. time. Error bars have, in most cases, the same size of the data points and they are calculated as previously described.

Table 1: χ^2, y_0, b and t_0 of the logistic fit for OD_{600nm}, QTx TOT and CFU ml^{-1}.

Logistic 3 parameters	OD_{600nm}	QTx TOT (# ml^{-1})	CFU ml^{-1}
χ^2	1.04	1.17	1.17
y_0	1.35 ± 0.01	(212 ± 8) × 10^7	(211 ± 6) × 10^7
b (min^{-1})	(3.3 ± 0.1) × 10^{-2}	(3.4 ± 0.5) × 10^{-2}	(5.2 ± 0.4) × 10^{-2}
t_0 (min)	128 ± 1	145 ± 5	151 ± 2

The b values of OD_{600nm} and QTx TOT are compatible within their uncertainties, and this result is expected since the OD_{600nm} is an indirect measurement of the total concentration of cells in suspension. The grow rate of CFU ml^{-1} is faster and the corresponding doubling time (about 19 minutes) is compatible with the value reported in the literature (Son M.S. et al, 2001).

2.3.2 Bacteria and experiments in ChAMBRe

To prepare the inoculum for the chamber experiments, the *E. coli* is grown in 30 ml of fresh TSB nonselective medium, in a shaking incubator at 37 °C and 200 rpm and its growth is followed by checking the OD_{600nm} value until the mid-exponential phase. When OD_{600nm} ~ 0.5, 20 ml of this liquid preparation is centrifuged at 3000 rpm for 10 min. Afterward, the bacteria pellet, separated by surnatant, is resuspended in 20 ml of sterile physiological solution (NaCl 0.9 % w/v) to prepare a suspension of approximately 10^8 CFU mL^{-1}, as verified by standard dilution plating. To retrieve the bacterial concentration, the average of CFU counting on agar plates and the uncertainty are calculated following the same metric described in 2.3.1 paragraph.

For the experiments performed at ChAMBRe, the typical bacterial concentration in the inoculum is 10^7 CFU ml^{-1}: to reach this concentration, a further dilution step is needed (i.e., typically 1:10 or 1:5) before the injection (see Massabò et al, 2018 for details).

The concentration of the solution to be injected inside ChAMBRe is also controlled in terms of total cells ml^{-1} by Quantom Tx Microbial Cell Counter. The sample is prepared from the bacterial suspension in physiological solution. In each single analysis, Quantom Tx acquires 10 visual fields of the slide's counting chamber, which correspond to an approx. volume of 0.09 µl, to retrieve the bacterial count. To evaluate if the exposure of Quantom Tx lamp degrades the fluorescent probe (photobleaching) of total cells, we repeated the total cell counts inserting and ejecting 10 times the same sample: the total count probe didn't show a particular sensitivity to the exposure to the

Quantom Tx lamp, and the coefficient of variation turned out to be less than 5%. Further details on the use of Quantom Tx counter are given in Supplement S4.

The bacteria suspension, properly diluted, is injected into the chamber volume mainly by using the Sparging Liquid Aerosol Generator, SLAG, which ensured the better reproducibility in earlier tests (Danelli et al., 2021). The injection phase typically lasts 5 minutes. Injection air flow and duration are automatically controlled by a Mass Flow Controller (Bronkhorst, model F201C-FA) managed via SCADA. In this way, 2 ml of bacterial suspension are nebulized inside ChAMBRe.

Experiments with *E. coli* have been performed by active sampling via the Andersen impactor: sampling time was progressively increased after the injection to collect a suitable number of CFUs. Sampling time during *E. coli* experiments are summarized in Table S2 in Supplement S5.

After the experiments in the simulation chamber, the plates sampled are incubated at 37 °C for 24 h. The CFUs are then counted and, in the experiments conducted by active sampling, the CFU cm^{-3} are calculated.

The possible correlation between bacteria viability and air quality can be investigated in terms of change in bacteria viability due to the exposure to atmospheric pollutants. Effects on bacteria viability are compared in relation to "baseline experiments". In a baseline experiment, the viability of airborne bacteria is measured at atmospheric pressure, with temperatures around 20°C and with relative humidity around 60%: such values have been chosen to reproduce an environment suitable for the survival of bacteria (Dunklin E.W. 1948; Cox C.S. 1966; Benbough J.E. 1967). During baseline experiments, the bacteria's viability depended on their characteristics and experimental procedures only. The baseline was assessed both in "dark" (solar simulator off) and "light" (solar simulator on) conditions. With "light" condition, the Solar Simulator was used with the AM1.5 filter mounted (see 2.1) to reduce the UV radiation; several experiments were replicated with the Solar Simulator lamp intensity set at 105% and 80% of the nominal value (i.e., the maximum and minimum intensity level which guarantees stability without using neutral filters). Baseline experiments, see Section 3, were particularly important also to assess the reproducibility and hence the sensitivity of the whole procedure.

The baseline assessment was followed by a set of exploratory experiments with E. *coli* exposed to selected pollutants. We measured the possible bacterial viability changes due to the exposure to atmospheric conditions typically met in polluted urban areas. So far, *E. col*i was exposed to

different concentrations of NO and NO_2, two of the most common pollutants emitted by vehicular and ship traffics (Seinfeld and Pandis, 1998; Monks et al., 2009; Pöschl and Shiraiwa, 2015;).

3. Results

The experiments performed to investigate the possible effects on bacteria viability due to the exposure to atmospheric pollutants, were conducted by following the same procedure adopted to assess the baseline and introducing inside ChAMBRe the specific pollutant. During gas pollutant experiments, NO or NO_2 concentration was kept constant thanks to the feedback control system described in *2.1.3*.

3.1 Baseline experiments with E. coli in dark conditions.

E. coli behavior in a set of eight replicated experiments, led from separate cultures, was first determined in dark conditions. The average total concentration and standard deviation of *E. coli* inside the chamber at t = 0 (three minutes after the conclusion of the injection to allow proper mixing/homogenization inside the ChAMBRe volume) was (0.34 ± 0.08) cells cm^{-3}, as measured by the WIBS; the average viable concentration and standard deviation, determined by the Andersen impactor sampling at t = 0 was (0.04 ± 0.02) cells cm^{-3}. The viable concentration at t = 0 was obtained by measuring the CFUs on three petri consecutively sampled; the coefficient of variation on the CFUs collected on the three petri, resulted equal to 12%.

The average ratio and standard deviation of viable:total (V:T in the following) bacteria concentration inside ChAMBRe, at t = 0 turned out to be V:T = (0.13 ± 0.07). The total and viable bacteria concentration values measured inside ChAMBRe depended on the V:T ratio in the inoculum to be injected (biological effects between each bacteria culture) and on the aerosolization process affecting the bacteria viability. The bacteria viable concentration in the inoculum was determined via standard dilution plating while the bacteria total concentration was calculated by the Quantom Tx. During baseline experiments, the V:T ratio of the inoculum ranged between 0.25 ± 0.03 and 0.50 ± 0.06. Time-trends of the averaged total and viable concentration of the bacteria, nebulized inside ChAMBRe, are shown in Figure 7. Bacteria lifetime in ChAMBRe can be calculated by fitting the data of each experiment with an exponential function as:

$$C(t) = C_0 e^{-\frac{t}{\tau}} \qquad (2)$$

where C_0 is the total or viable concentration of *E. coli* just after the injection (t = 0) and τ is the total or viable bacteria lifetime, respectively. In table 2, the average and standard deviation of C_0 and τ for the *E. coli* total and viable concentration of eight experiments are reported.

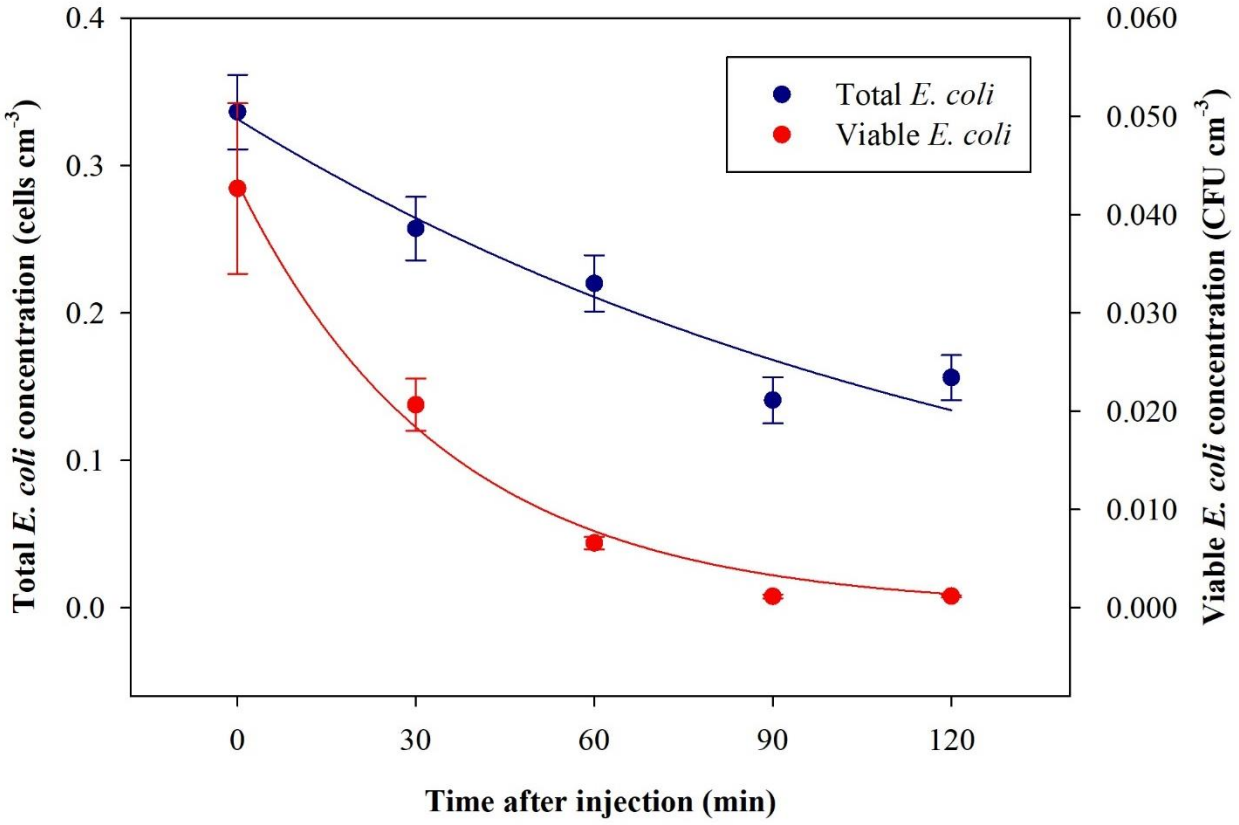

Figure 7: Time-trend of *E. coli* average bacteria total (blue) and viable (red) concentration inside ChAMBRe obtained by eight repetitions of baseline experiments.

Table 2: C_0 and τ (average ± std deviation) of the exponential fit for total and viable concentration of *E. coli*.

Exponential function	Total *E. coli*	Viable *E. coli*
C_0	(0.33 ± 0.08) cells cm^{-3}	(0.04 ± 0.02) CFU cm^{-3}
τ (min)	153 ± 22	32 ± 5

The total *E. coli* averaged lifetime is about 153 minutes; this value agrees with data reported in (Massabò et al., 2018) for generic aerosols: particles in the same size range of *E. coli* (1-2 μm) and τ =2-3 hours. The viable *E. coli* averaged lifetime is about 32 minutes, lower than the aerodynamic lifetime, this indicating the difficulty of this microorganism to survive in the atmospheric medium.

3.2 Experiments with E. coli and NOx in dark conditions.

A preliminary check was performed exposing the *E. coli* to O_3, which is recognized to be a strong antimicrobial agent (Kim et al., 1999; Giuliani et al., 2018; Thanomsub et al., 2022), hence the expected result was a complete viability loss. The exposure of bacteria to O_3 (concentration > 1000 ppb) resulted in a complete cell mortality, as expected. The initial condition immediately after the injection was V:T = (0.03 ± 0.01) and no CFUs were collected in any of the following samplings (starting 30 minutes after the injection).

In another experiment, bacteria were exposed to NO_2 and NO concentrations, 900 and 1200 ppb for both the pollutants. The exposure of bacteria to such pollutants showed a V:T reduction. The average results, obtained in a set of eight experiments, led from separate cultures, are shown in Figure 8.

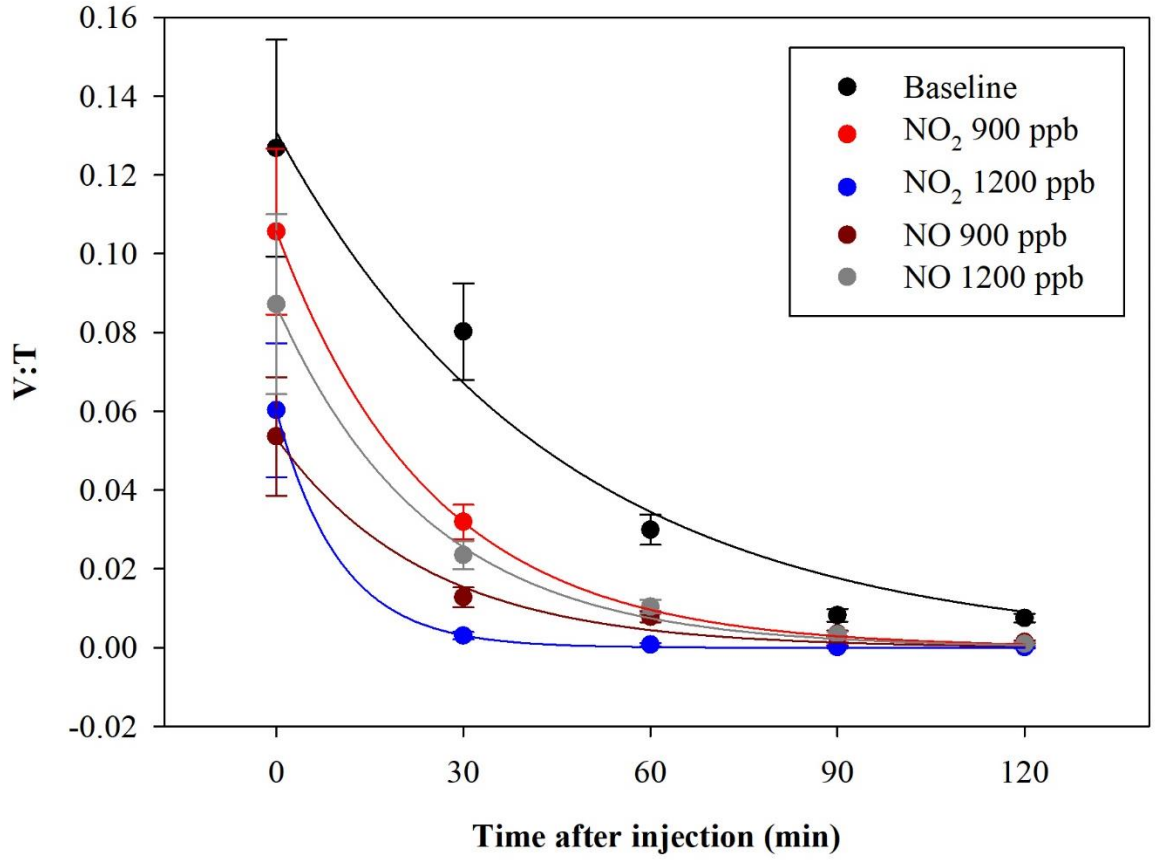

Figure 8: Time-trend of the V:T ratio for E. coli in baseline (black) and in the experiments with ChAMBRe maintained at a constant concentration of: NO_2 (900 ppb red and 1200 ppb blue) and NO (900 ppb dark red and 1200 ppb gray).

The quantitative reduction in the *E. coli* lifetime, due to the exposure to pollutants, can be evaluated considering the V:T ratio and fitting the data with an exponential curve, as previously described; the results are shown in Table 3.

Table 3: Initial values and τ (average and std deviation) of the exponential fit for V:T ratio of *E. coli* at different pollutants concentrations.

Exponential function	(V:T t = 0)	τ (min)	experiments #
Baseline	0.13 ± 0.07	40 ± 5	8
NO_2 900 ppb	0.11 ± 0.02	25 ± 2	2
NO_2 1200 ppb	0.06 ± 0.02	11 ± 2	2
NO 900 ppb	0.05 ± 0.01	26 ± 3	2
NO 1200 ppb	0.10 ± 0.02	25 ± 4	2

E. coli averaged lifetime in baseline experiments, calculated on the V:T ratio, turned out to be about 40 min. The exposure of E. coli to NO_2 reduced the lifetime to about 25 and 11 min with a concentration of 900 ppb and 1200 ppb respectively. The exposure to 900 ppb and 1200 ppb of NO decreased bacteria lifetime to 26 and 25 min, respectively and the values are similar to the value obtained with the lowest NO_2 concentration. The increase of the NO concentration did not correspond to a decrease in the E. coli viability, as observed with NO_2: these results suggest a greater toxic effect of NO_2 than of NO on E. coli. The literature of a comparison of the toxic effects of NO and NO_2 on *E coli* is poor. Some research articles have demonstrated negative effects of these two gases on bacterial strains: Kosaka et al 1986 found a decrease in *E. coli* viability with increasing NO_2 concentration. Janvier et al, 2020 highlighted a significant adverse effect of NO_2 on some commensal skin bacterial strains. Mancinelli and McKay, 1983 found that a low concentration of NO is bacteriostatic for some organisms but not for others. It is worth noting that NO has a strong antimicrobial property, being an endogenously produced molecule that is critical for critical infection defence (Fang, 1997), although some bacteria are able to escape this NO action (Privett et al., 2012).

3.2 Experiments with E. coli and Solar Simulator.

E. coli behavior when exposed to light was determined in a set of dedicated baseline experiments. No significant differences in results appeared changing the intensity of the Solar Simulator operated with the AM1.5G filter and the data with a Solar Simulator intensity of 100% are here reported. After the injection, the average total concentration of *E. coli* reached inside the chamber was (0.30 ± 0.03) cells cm^{-3}, compatible with the dark baseline; while the average viable concentration was (0.019 ± 0.005) cells cm^{-3}, lower than what obtained in dark experiments. The consequent V:T ratio was (0.06 ± 0.02). The viable concentration collapses quickly, reaching zero after 30 minutes. The comparison between V:T ratio obtained for dark and light baseline is shown in Figure 9.

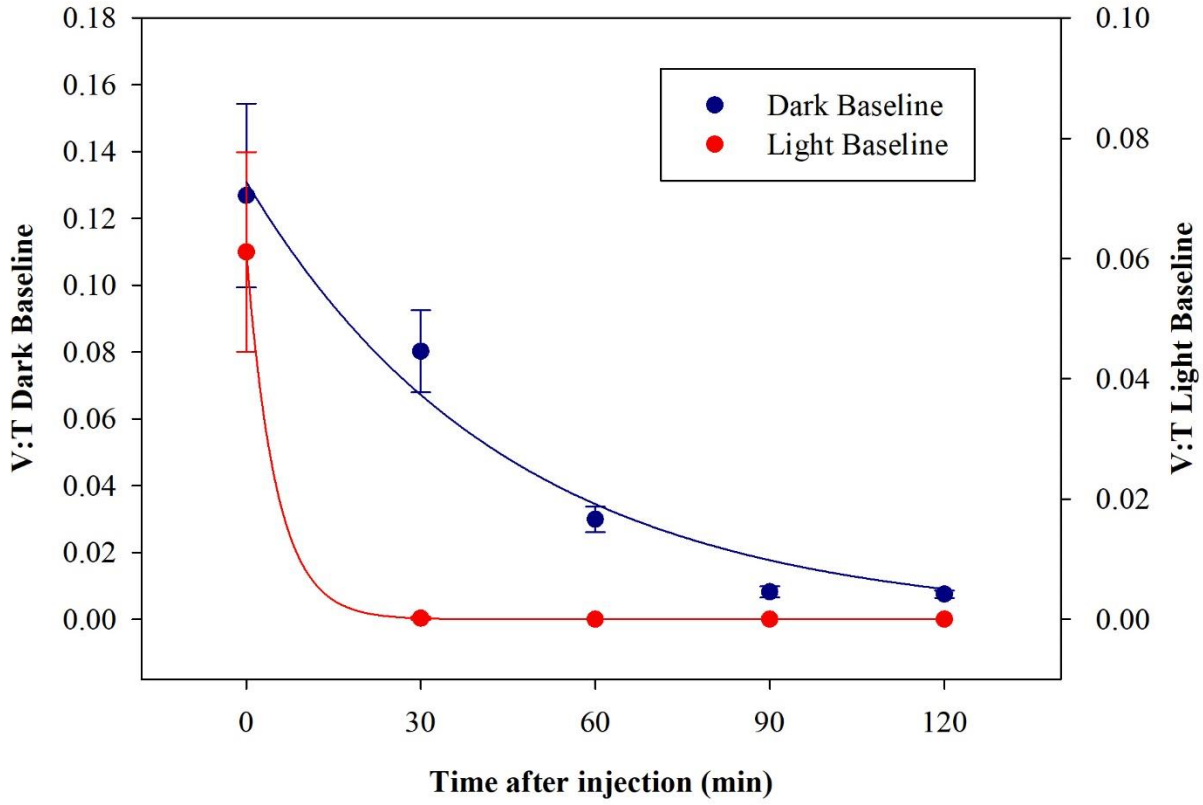

Figure 9: Time-trend of the V:T ratio for E. coli in the dark baseline (dark blue) and light baseline (red) experiments.

These results indicate a significant decrease in bacteria viability due to their exposure to solar radiation. The behavior, here evaluated in atmospheric environment, agrees with observation in water environments reported in several works (Whitman et al., 2004; Jozić et al., 2014; Tiwari et

al., 2022); the solar radiation is indicated as an abiotic factor with the negative effect of bringing some bacteria strains, among which *E. coli*, into a temporary inactivation/non-cultivable state.

4. Discussion, conclusion and perspectives

The main result presented in this work is the assessment of a multi-step and well controlled protocol to perform experiments on the impact of air quality on bacteria viability by an atmospheric simulation chamber, ChAMBRe in this case. Even if the chamber configuration is still in progress and several new equipment will be deployed at ChAMBRe in the near future, the present set-up opens the possibility of systematic studies. The average τ of the V:T ratio of eight baseline experiments was 40 min with a standard deviation of 5 min; the coefficient of variation of 13% corresponds to the experimental sensitivity to changes in *E. coli* viability due to exposure to pollutants and/or other relevant parameters. The baseline reference must be experimentally determined for each bacteria strain and efforts are planned for repeating the observation with *Bacillus subtilis*, *Bacillus spizizenii* and *Pseudomonas fluorescens* in the near future. It is worthy to note that the experimental protocol returns the lifetime of total and viable bacteria injected in the chamber. The figure for total bacteria corresponds to the aerodynamic behavior of aerosol of diameter around 1 μm, already reported in (Massabò et al., 2008) while the lifetime of viable bacteria is much shorter (about half an hour) due to the difficulty of this microorganism to survive in the atmospheric medium. Such shorter lifetime posed clear constraints on the first experiments with exposure of *E. coli* to NO_x inside ChAMBRe. A time window of two hours after the bacteria injection was considered to observe the behavior of *E. coli* viability and it was possible to quantify a lifetime reduction, in dark conditions, clearly related to NO and NO_2 concentration inside ChAMBRe. These findings pave the road to systematic studies including other bacteria strains and pollutant species. With the *E. coli* exposed to the light produced by the Solar Simulator operated with the AM1.5 filter, the viability resulted very short even in the baseline conditions and therefore no further experiment with pollutants was performed. With other bacterial strains, the impact of light on viability will have to be reinvestigated.

It is well known in the literature that the viable but non-culturable condition (VBNC) is a survival strategy of many bacteria in the environment in response to adverse environmental conditions (e.g., solar radiation). There is a growing scientific interest in studying VBNC cells, including to understand novel public health implications of VBNC cells. In our simulated experiments, we are

investigating alternative methods to detect bacterial viability and VBNC state, such as “live and dead staining” by fluorescence microscopy. This assay can be used to monitor the viability of bacterial populations as a function of cell membrane integrity using different fluorescent dyes. Further experiments with “flow cytometry” could certainly be more beneficial not only to enumerate live and dead bacteria, but also to evaluate the health and viability of bacterial cells by determining the activity of bacterial oxidases and reductases.

5. Acknowledgments

We are indebted to the personnel of the mechanical workshop of the INFN division of Genoa for the continuous support in the development of the ChAMBRe structure. The development of the chamber and the deployment of the equipment was supported by several European and Italian projects/grants: EUROCHAMP2020 (H2020: Infrastructure Activity under grant agreement No 730997); PON per-ACTRIS-IT (MUR-IT: PON project PIR_00015 “Per ACTRIS IT”); BLUE-LAB NET (F.E.S.R. - FONDO EUROPEO DI SVILUPPO REGIONALE Azione POR, Regione Liguria, IT); ATMO-ACCESS (H2020: Infrastructure Activity under grant agreement No 101008004); NextGenerationEU PNRR-ITINERIS (Italian Integrated Environmental Research Infrastructures System). The publication has been funded by EU - Next Generation EU Mission 4 “Education and Research” - Component 2: “From research to business” - Investment 3.1: “Fund for the realisation of an integrated system of research and innovation infrastructures” - Project IR0000032 – ITINERIS - Italian Integrated Environmental Research Infrastructures System - CUP B53C22002150006. The authors acknowledge the Research Infrastructures participating in the ITINERIS project with their Italian nodes: ACTRIS, ANAEE, ATLaS, CeTRA, DANUBIUS, DISSCO, e-LTER, ECORD, EMPHASIS, EMSO, EUFAR, Euro-Argo, EuroFleets, Geoscience, IBISBA, ICOS, JERICO, LIFEWATCH, LNS, N/R Laura Bassi, SIOS, SMINO.

6. References

Akin, E., Pelen, N. N., Tiryaki, I. U., Yalcin, F.: Parameter identification for gompertz and logistic dynamic equations, PLoSONE15(4): e0230582, https://doi.org/10.1371/journal.pone.0230582, 2020.

Amato, P., Demeer, F., Melaouhi, A., Fontanella, S., Martin-Biesse, A.-S., Sancelme, M., Laj, P., Delort, A.-M.: A fate for organic acids, formaldehyde and methanol in cloud water: their biotransformation by micro-organisms, Atmospheric Chem. Phys. 7, 4159–4169, 2007.

Amato, P., Joly, M., Schaupp, C., Attard, E., Möhler, O., Morris, C.E., Brunet, Y., Delort, A.-M.: Survival and ice nucleation activity of bacteria as aerosols in a cloud simulation chamber, Atmospheric Chem. Phys. 15, 6455–6465. https://doi.org/10.5194/acp-15-6455-2015, 2015.

Amato, P., Mathonat, F., Nuñez Lopez, L., Péguilhan, R., Bourhane, Z., Rossi, F., Vyskocil, J., Joly, M., and Ervens, B.: The aeromicrobiome: the selective and dynamic outer-layer of the Earth's microbiome, Frontiers in Microbiology, 14, https://doi.org/10.3389/fmicb.2023.1186847, 2023

Annadurai, G., Rajesh Babu, S., Srinivasamoorthy, V. R.: Development of mathematical models (Logistic, Gompertz and Richards models) describing the growth pattern of Pseudomonas putida (NICM 2174), Bioprocess Engineering, 23(6), 607-612, https://doi.org/10.1007/s004490000209, 2000.

Ariya, P.A., Amyot, M.: New Directions: The role of bioaerosols in atmospheric chemistry and physics, Atmos. Environ. 38, 1231–1232, https://doi.org/10.1016/j.atmosenv.2003.12.006, 2004.

Baty, F., Delignette-Muller, M. L. : Estimating the bacterial lag time : which model, which precision?, International journal of food microbiology, 91(3), 261-277, https://doi.org/10.1016/j.ijfoodmicro.2003.07.002, 2004.

Bauer, H., Giebl, H., Hitzenberger, R., Kasper-Giebl, A., Reischl, G., Zibuschka, F., Puxbaum, H.: Airborne bacteria as cloud condensation nuclei, Journal of Geophysical Research, vol. 108, no. D21, 4658, doi:10.1029/2003JD003545, 2003.

Benbough, J. E.: Death Mechanisms in Airborne *Escherichia coli,* J. Gen. Microbiol. 47, 325–333, https://doi.org/10.1099/00221287-47-3-325, 1967.

Birch, C. P. D.: A new generalized logistic sigmoid growth equation compared with the Richards growth equation, Annals of botany, 83(6), 713-723, https://doi.org/10.1006/anbo.1999.0877, 1999.

Brotto, P., Repetto, B., Formenti, P., Pangui, E., Livet, A., Bousserrhine, N., Martini, I., Varnier, O., Doussin, J.F., Prati, P.: Use of an atmospheric simulation chamber for bioaerosol investigation: a feasibility study, Aerobiologia 31, 445–455, https://doi.org/10.1007/s10453-015-9378-2, 2015.

Bundke, U., Reimann, B., Nillius, B., Jaenicke, R., Bingemer, H.: Development of a Bioaerosol single particle detector (BIO IN) for the Fast Ice Nucleus CHamber FINCH, Atmos. Meas. Tech., 3, 263–271, https://doi.org/10.5194/amt-3-263-2010, 2010.

Burrows, S. M., Butler, T., Jöckel, P., Tost, H., Kerkweg, A., Pöschl, U., Lawrence, M.G.: Bacteria in the global atmosphere – Part 2: Modeling of emissions and transport between different ecosystems, Atmospheric Chem. Phys. 9, 9281–9297. https://doi.org/10.5194/acp-9-9281-2009, 2009.

741 Chou, C., Stetzer, O., Weingartner, E., Jurányi, Z., Kanji, Z. A., Lohmann, U.: Ice nuclei properties
742 within a Saharan dust event at the Jungfraujoch in the Swiss Alps, Atmos. Chem. Phys., 11, 4725–
743 4738, https://doi.org/10.5194/acp-11-4725-2011, 2011.

744 CID, Commission Implementing Decision (EU) 2023/900, "Setting up the Aerosol, Clouds and
745 Trace Gases Research Infrastructure (ACTRIS ERIC)" Official Journal of the European Union
746 L115/15, 03/05/2023.

747 Cox, C.S.: The Survival of *Escherichia coli* sprayed into Air and into Nitrogen from Distilled
748 Water and from Solutions of Protecting Agents, as a Function of Relative Humidity, J. Gen.
749 Microbiol. 43, 383–399, https://doi.org/10.1099/00221287-43-3-383, 1966.

750 Danelli, S., Brunoldi, M., Massabò, D., Parodi, F., Vernocchi, V., Prati, P.: Comparative
751 characterization of the performance of bio-aerosol nebulizers in connection with atmospheric
752 simulation chambers. Atmos. Meas. Tech., 14, 4461–4470, https://doi.org/10.5194/amt-14-4461-
753 2021, 2021.

754 Deguillaume, L., Leriche, M., Amato, P., Ariya, P.A., Delort, A.-M., Pöschl, U., Chaumerliac, N.,
755 Bauer, H., Flossmann, A.I., Morris, C.E.: Microbiology and atmospheric processes: chemical
756 interactions of primary biological aerosols, Biogeosciences 5, 1073–1084,
757 https://doi.org/10.5194/bg-5-1073-2008, 2008.

758 Delort, A. M., Vaïtilingom, M., Amato, P., Sancelme, M., Parazols, M., Mailhot, G., Laj, P.,
759 Deguillaume, L.: A short overview of the microbial population in clouds: Potential roles in
760 atmospheric chemistry and nucleation processes, Atmospheric Research, Volume 98, Issues 2–4,
761 Pages 249-260, https://doi.org/10.1016/j.atmosres.2010.07.004, 2010.

762 Després, V. R., Huffman, J. A., Burrows, S. M., Hoose, C., Safatov, A. S., Buryak, G., Fröhlich-
763 Nowoisky, J., Elbert, W., Andreae, M.O., Pöschl, U., Jaenicke, R.: Primary biological aerosol
764 particles in the atmosphere: a review. Tellus B Chem. Phys. Meteorol. 64, 15598,
765 https://doi.org/10.3402/tellusb.v64i0.15598, 2012.

766 Dunklin, E. W., Puck, T. T.: The lethal effect of relative humidity on airborne bacteria. J. Exp.
767 Med. 87, 87–101, https://doi.org/10.1084/jem.87.2.87, 1948.

768 Ehrlich, R., Miller, S., and Walker, R. L.: Relationship Between Atmospheric Temperature and
769 Survival of Airborne Bacteria, Appl Microbiol, 19, 245–249, 1970.

770 Ervens, B. and Amato, P.: The global impact of bacterial processes on carbon mass. Atmos. Chem.
771 Phys., 20, 1777–1794, https://doi.org/10.5194/acp-20-1777-2020, 2020.

772 Fang, F. C.: Perspectives series: host/pathogen interactions. Mechanisms of nitric oxide-related
773 antimicrobial activity, J Clin Invest. 99(12): 2818–2825, https://doi.org/10.1172%2FJCI119473,
774 1997.

775 Fankhauser, A. M., Antonio, D. D., Krell, A. M., Alston, S. J., Banta, S., and McNeill, V. F.:
776 Constraining the impact of bacteria on the aqueous atmospheric chemistry of small organic
777 compounds, ACS Earth Space Chem., https://doi.org/10.1021/acsearthspacechem.9b00054, 2019.

778 Fröhlich-Nowoisky, J., Kampf, C. J., Weber, B., Huffman, J. A., Pöhlker, C., Andreae, M. O.,
779 Lang-Yona, N., Burrows, S. M., Gunthe, S. S., Elbert, W., Su, H., Hoor, P., Thines, E., Hoffmann,
780 T., Després, V. R., Pöschl, U.: Bioaerosols in the Earth system: Climate, health, and ecosystem
781 interactions. Atmospheric Res. 182, 346–376, https://doi.org/10.1016/j.atmosres.2016.07.018,
782 2016.

783 Giuliani, G., Ricevuti, G., Galoforo, A., Franzini, M.: Microbiological aspects of ozone:
784 bactericidal activity and antibiotic/antimicrobial resistance in bacterial strains treated with ozone.
785 Ozone Therapy, 3(3), https://doi.org/10.4081/ozone.2018.7971, 2018.

786 Gong, J., Qi, J., E, B., Yin, Y., Gao, D.: Concentration, viability and size distribution of bacteria
787 in atmospheric bioaerosols under different types of pollution. Environmental Pollution 257,
788 113485, https://doi.org/10.1016/j.envpol.2019.113485, 2020.Hall, B. G., Acar, H., Nandipati, A.,
789 Barlow, M.: Growth Rates Made Easy, Mol. Biol. Evol. 31, 232–238,
790 https://doi.org/10.1093/molbev/mst187, 2014.

791 Jaber, S., Lallement, A., Sancelme, M., Leremboure, M., Mailhot, G., Ervens, B., and Delort, A.-
792 M.: Biodegradation of phenol and catechol in cloud water: comparison to chemical oxidation in
793 the atmospheric multiphase system, Atmospheric Chemistry and Physics, 20, 4987–4997,
794 https://doi.org/10.5194/acp-20-4987-2020, 2020.

795 Jaber, S., Joly, M., Brissy, M., Leremboure, M., Khaled, A., Ervens, B., and Delort, A.-M.: Biotic
796 and abiotic transformation of amino acids in cloud water: experimental studies and atmospheric
797 implications, Biogeosciences, 18, 1067–1080, https://doi.org/10.5194/bg-18-1067-2021, 2021.

798 Jang, J., Hur, H.-G., Sadowsky, M. J., Byappanahalli, M. N., Yan, T., Ishii, S.: Environmental
799 *Escherichia coli*: ecology and public health implications-a review, J. Appl. Microbiol. 123, 570–
800 581, https://doi.org/10.1111/jam.13468, 2017.

801 Janvier, X., Alexandre, S., Boukerb, A. M., Souak, D., Maillot, O., Barreau, M., Gouriou, F.,
802 Grillon, C., Feuilloley, M. G. J., Groboillot, A.: Deleterious Effects of an Air Pollutant (NO_2) on
803 a Selection of Commensal Skin Bacterial Strains, Potential Contributor to Dysbiosis?, Frontiers of
804 in Microbiology, Volume 11, Article 591839, https://doi.org/10.3389/fmicb.2020.591839, 2020.
805

806 Jozić, S., Morović, M., Šolić, M., KrstuIović, N., Ordulj, M.: Effect of solar radiation, temperature
807 and salinity on the survival of two different strains of *Escherichia coli*, Fresenius Environ. Bull.
808 23, 1852–1859, 2014.

809 Khaled, A., Zhang, M., Amato, P., Delort, A.-M., and Ervens, B.: Biodegradation by bacteria in
810 clouds: an underestimated sink for some organics in the atmospheric multiphase system,
811 Atmospheric Chemistry and Physics, 21, 3123–3141, https://doi.org/10.5194/acp-21-3123-2021,
812 2021.

813 Krumins, V., Mainelis, G., Kerkhof, L. J., and Fennell, D. E.: Substrate-Dependent rRNA
814 Production in an Airborne Bacterium, Environ. Sci. Technol. Lett., 1, 376–381,
815 https://doi.org/10.1021/ez500245y, 2014.

816 Kim, J. G., Yousef, A. E., Dave, S.: Application of Ozone for Enhancing the Microbiological
817 Safety and Quality of Foods: A Review, Journal of Food Protection, 62, 9, 1071-1087,
818 https://doi.org/10.4315/0362-028X-62.9.1071, 1999.

819 Kolbe, U., Yi, B., Poth, T., Saunders, A., Boutin, S., Dalpke, A. H.: Early Cytokine Induction
820 Upon Pseudomonas aeruginosa Infection in Murine Precision Cut Lung Slices Depends on Sensing
821 of Bacterial Viability, Frontiers in Immunology 2020, 11:598636,
822 https://doi.org/10.3389/fimmu.2020.598636, 2020.

823 Kosaka, H., Yamamoto, H., Oda, Y., Uozumi, M: Induction of SOS functions by nitrogen dioxide
824 in Escherichia coli with different DNA-repair capacities, Mutat Res. Aug; 162(1):1-5, doi:
825 10.1016/0027-5107(86)90065-5, 1986.

826 Lee, B. U., Kim, S. H., Kim, S. S.: Hygroscopic growth of *E. coli* and *B. subtilis* bioaerosols,
827 Journal of Aerosol Science 33, 1721–1723, https://doi.org/10.1016/S0021-8502(02)00114-3,
828 2002.

829 Lee, B. U., Kim, S. S.: Sampling *E. coli* and *B. subtilis* bacteria bioaerosols by a new type of
830 impactor with a cooled impaction plate, J. Aerosol Sci., 34, 1097–1100, 2003.

831 Lieberherr, G., Auderset, K., Calpini, B., Clot, B., Crouzy, B., Gysel-Beer, M., Konzelmann, T.,
832 Manzano, J., Mihajlovic, A., Moallemi, A., O'Connor, D., Sikoparija, B., Sauvageat, E., Tummon,
833 F., Vasilatou, K: Assessment of real-time bioaerosol particle counters using reference chamber
834 experiments, Atmos. Meas. Tech., 14, 7693–7706, https://doi.org/10.5194/amt-14-7693-2021,
835 2021.

836 Lighthart, B., Shaffer, B.T., Marthi, Ganio, L. M.: Artificial wind-gust liberation of microbial
837 bioaerosols previously deposited on plants. Aerobiologia 9, 189–196,
838 https://doi.org/10.1007/BF02066261, 1993.

839 Mancinelli, R. L. and McKay, C.P.: Effects of Nitric Oxide and Nitrogen Dioxide on Bacterial
840 Growth, Applied and Environmental Microbiology, 198-202,
841 https://doi.org/10.1128/aem.46.1.198-202.1983, 1983.

842 Mainelis, G., Berry, D., Reoun An, H., Yao, M., DeVoe, K., Fennell, D.E., Jaeger, R.: Design and
843 performance of a single-pass bubbling bioaerosol generator, Atmos. Environ. 39, 3521– 3533,
844 https://doi.org/10.1016/j.atmosenv.2005.02.043, 2005.

845 Martiny, J. B. H., Bohannan, B. J. M., Brown, J. H., Colwell, R. K., Fuhrman, J. A., Green, J. L.,
846 Horner-Devine, M. C., Kane, M., Krumins, J. A., Kuske, C. R., Morin, P. J., Naeem, S., Ovreås,
847 L., Reysenbach, A.-L., Smith, V. H., Staley, J. T.: Microbial biogeography: putting
848 microorganisms on the map. Nat. Rev. Microbiol. 4, 102–112,
849 https://doi.org/10.1038/nrmicro1341, 2006.

850 Massabò, D., Danelli, S. G., Brotto, P., Comite, A., Costa, C., Di Cesare, A., Doussin, J. F.,
851 Ferraro, F., Formenti, P., Gatta, E., Negretti, L., Oliva, M., Parodi, F., Vezzulli, L., Prati, P.:
852 ChAMBRe: a new atmospheric simulation chamber for aerosol modelling and bio-aerosol
853 research, Atmos. Meas. Tech., 11, 5885–5900, https://doi.org/10.5194/amt-11-5885-2018, 2018.

Mayol, E., Jiménez, M. A., Herndl, G. J., Duarte, C. M., and Arrieta, J. M.: Resolving the abundance and air-sea fluxes of airborne microorganisms in the North Atlantic Ocean. Frontiers in Microbiology, 5, https://doi.org/10.3389/fmicb.2014.00557, 2014.

Möhler, O., DeMott, P. J., Vali, G., Levin, Z.: Microbiology and atmospheric processes: the role of biological particles in cloud physics, Biogeosciences 4, 1059–1071, https://doi.org/10.5194/bg-4-1059-2007, 2007.

Monks, P. S., Granier, C., Fuzzi, S., Stohl, A., Williams, M. L., Akimoto, H., Amann, M., Baklanov, A., Baltensperger, U., Bey, I., Blake, N., Blake, R. S., Carslaw, K., Cooper, O. R., Dentener, F., Fowler, D., Fragkou, E., Frost, G. J., Generoso, S., Ginoux, P., Grewe, V., Guenther, A., Hansson, H. C., Henne, S., Hjorth, J., Hofzumahaus, A., Huntrieser, H., Isaksen, I. S. A., Jenkin, M. E., Kaiser, J., Kanakidou, M., Klimont, Z., Kulmala, M., Laj, P., Lawrence, M. G., Lee, J. D., Liousse, C., Maione, M., McFiggans, G., Metzger, A., Mieville, A., Moussiopoulos, N., Orlando, J. J., O'Dowd, C. D., Palmer, P. I., Parrish, D. D., Petzold, A., Platt, U., Pöschl, U., Prévôt, A. S. H., Reeves, C. E., Reimann, S., Rudich, Y., Sellegri, K., Steinbrecher, R., Simpson, D., ten Brink, H., Theloke, J., van der Werf, G. R., Vautard, R., Vestreng, V., Vlachokostas, Ch., von Glasow, R.: Atmospheric composition change – global and regional air quality, Atmos. Environ. 43, 5268–5350, https://doi.org/10.1016/j.atmosenv.2009.08.021, 2009.

Morris, C. E., Georgakopoulos, D. G., Sands, D. C.: Ice nucleation active bacteria and their potential role in precipitation. J. Phys. IV Proc. 121, 87–103, https://doi.org/10.1051/jp4:2004121004, 2004.

Morris, C. E., Leyronas, C., Nicot, P. C.: Movement of Bioaerosols in the Atmosphere and the Consequences for Climate and Microbial Evolution, in: Colbeck, I., Lazaridis, M. (Eds.), Aerosol Science: Technology and Applications. John Wiley & Sons, Ltd, Chichester, UK, pp. 393–415, https://doi.org/10.1002/9781118682555.ch16, 2014.

Mytilinaios, I., Salih, M., Schofield, H. K., Lambert, R. J. W.: Growth curve prediction from optical density data, Int. J. Food Microbiol. 154, 169–176, https://doi.org/10.1016/j.ijfoodmicro.2011.12.035, 2012.

Pöschl, U.: Atmospheric Aerosols: Composition, Transformation, Climate and Health Effects, Angew. Chem. Int. Ed. 44, 7520–7540, https://doi.org/10.1002/anie.200501122, 2005.

Pöschl, U., Shiraiwa, M.: Multiphase Chemistry at the Atmosphere–Biosphere Interface Influencing Climate and Public Health in the Anthropocene, Chem. Rev. 115, 4440–4475, https://doi.org/10.1021/cr500487s, 2015.

Privett, B. J., Broadnax, A. D., Bauman, S. J., Riccio, D. A., Schoenfisch, M. H.: Examination of bacterial resistance to exogenous nitric oxide, Nitric Oxide, Volume 26, Issue 3, Pages 169-173, https://doi.org/10.1016/j.niox.2012.02.002, 2012.

Romano, S., Di Salvo, M., Rispoli, G., Alifano, P., Perrone, M. R., Talà, A.: Airborne bacteria in the Central Mediterranean: Structure and role of meteorology and air mass transport, Science of the Total Environment 697 (2019) 134020, https://doi.org/10.1016/j.scitotenv.2020.138899, 2019.

Seinfeld, J. H., Pandis, S. N.: 1998. Atmospheric Chemistry and Physics: From Air Pollution to Climate Change, Wiley-Interscience, ISBN 10: 0471178152 ISBN 13: 9780471178156, 1997.

Shaffer, B.T., Lighthart, B.: Survey of Culturable Airborne Bacteria at Four Diverse Locations in Oregon: Urban, Rural, Forest, and Coastal, Microb. Ecol. 34, 167–177, https://doi.org/10.1007/s002489900046, 1997.

Son, M. S., Taylor R. K.: Growth and Maintenance of *Escherichia coli* Laboratory Strains, Curr. Protoc. 2021 January; 1(1): e20, https://doi.org/10.1002/cpz1.20, 2021.

Sun, J., Ariya, P.: Atmospheric organic and bio-aerosols as cloud condensation nuclei (CCN): A review, Atmos. Environ. 40, 795–820, https://doi.org/10.1016/j.atmosenv.2005.05.052, 2006.

Thanomsub, B., Anupunpisit, V., Chanphetch, S., Watcharachaipong, T., Poonkhum, R., and Srisukonth, C.: Effects of ozone treatment on cell growth and ultrastructural changes in bacteria, J. Gen. Appl. Microbiol., 48, 193–199, https://doi.org/10.2323/jgam.48.193, 2002.

Tjørve, K. M. C., Tjørve, E.: The use of Gompertz models in growth analyses, and new Gompertz-model approach: An addition to the Unified-Richards family, PLOS ONE June 5, 2017, https://doi.org/10.1371/journal.pone.0178691, 2017.

Tiwari, A., Kauppinen, A., Räsänen, P., Salonen, J., Wessels, L., Juntunen, J., Miettinen, I. T., Pitkänen, T.: Effects of temperature and light exposure on the decay characteristics of fecal indicators, norovirus, and Legionella in mesocosms simulating subarctic river water, Sci. Tot. Env. 859, https://doi.org/10.1016/j.scitotenv.2022.160340, 2022.

Vernocchi, V., Brunoldi, M., Danelli, S. G., Parodi, F., Prati, P., Massabò, D.: Characterization of soot produced by the mini-inverted soot generator with an atmospheric simulation chamber, Atmos. Meas. Tech., 15, 2159–2175, https://doi.org/10.5194/amt-15-2159-2022, 2022.

Wagstrom, K. M., Pandis, S. N., Yarwood, G., Wilson, G. M., Morris, R. E.: Development and application of a computationally efficient particulate matter apportionment algorithm in a three-dimensional chemical transport model. Atmos. Environ. 42 (2008) 5650–5659, https://doi.org/10.1016/j.atmosenv.2008.03.012, 2008.

Wang, C.-C., Fang, G.-C., Lee, L.: Bioaerosols study in central Taiwan during summer season, Toxicol. Ind. Health 23, 133–139, https://doi.org/10.1177/0748233707078741, 2007.

Whitman, R. L., Nevers, M. B., Korinek, G.C., Byappanahalli, M.N.: Solar and temporal effects on *Escherichia coli* concentration at a Lake Michigan swimming beach, Appl Environ Microbiol. Vol 70, No. 7, https://doi.org/10.1128/AEM.70.7.4276-4285.2004, 2004.

Wright, D. N., Bailey, G. D., and Goldberg, L. J.: Effect of Temperature on Survival of Airborne Mycoplasma pneumoniae, J Bacteriol, 99, 491–495, 1969.

Zwietering, M. H., Jongenburger, I., Rombouts, F. M., van 't Riet, K.: Modeling of the bacterial growth curve, Appl Environ Microbiol. 1990 Jun; 56(6): 1875–1881, DOI: https://doi.org/10.1128/aem.56.6.1875-1881.1990, 1990.